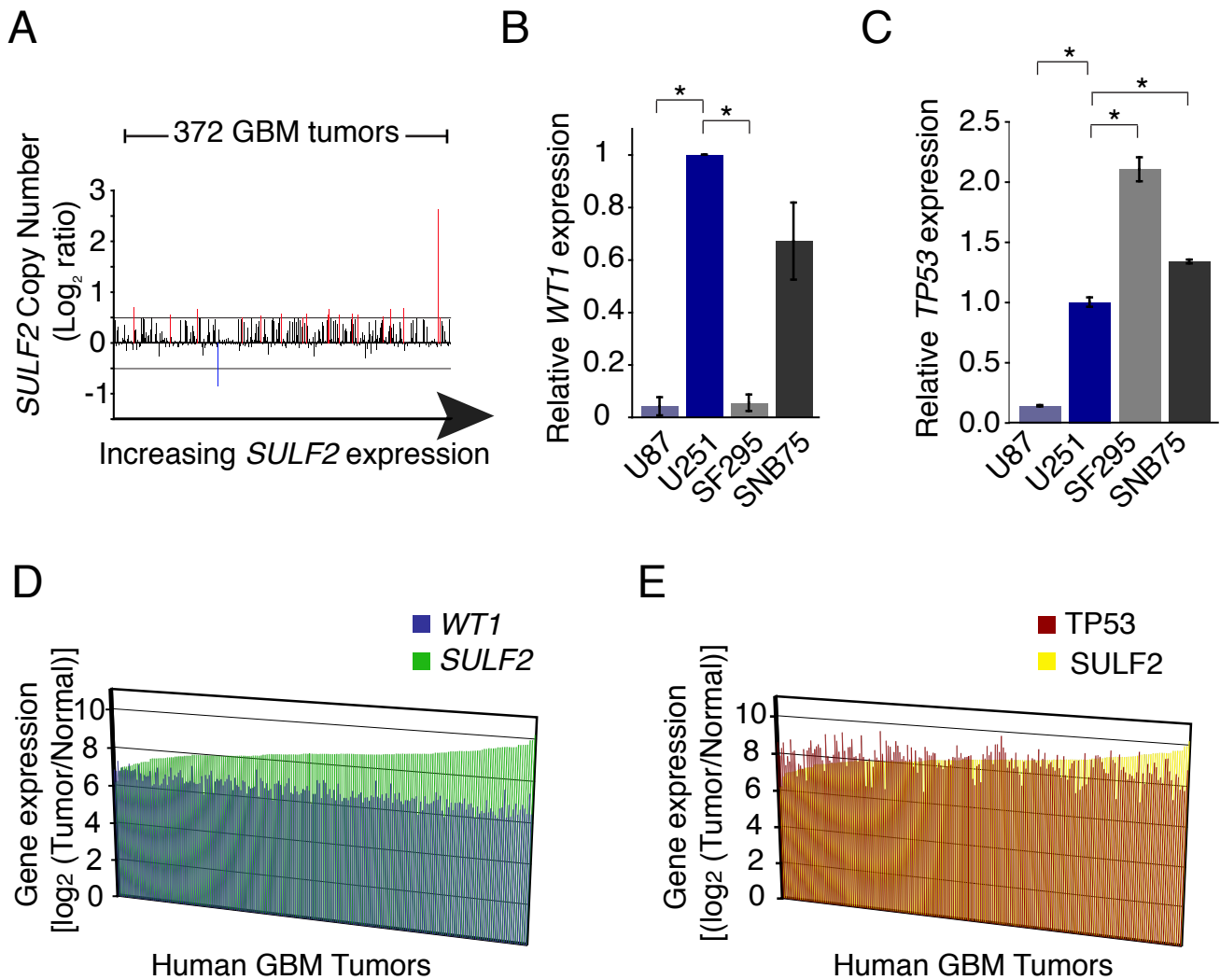
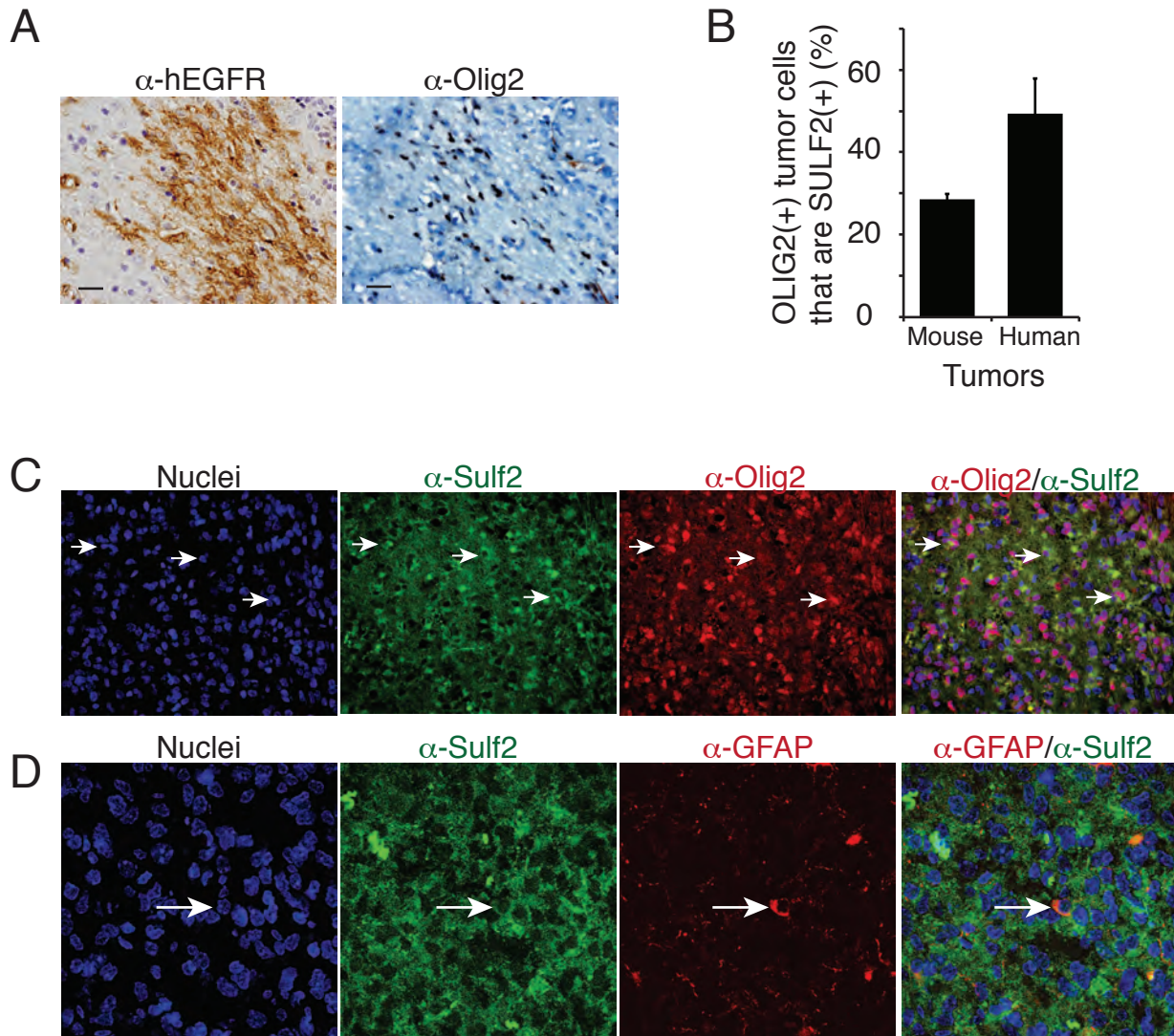


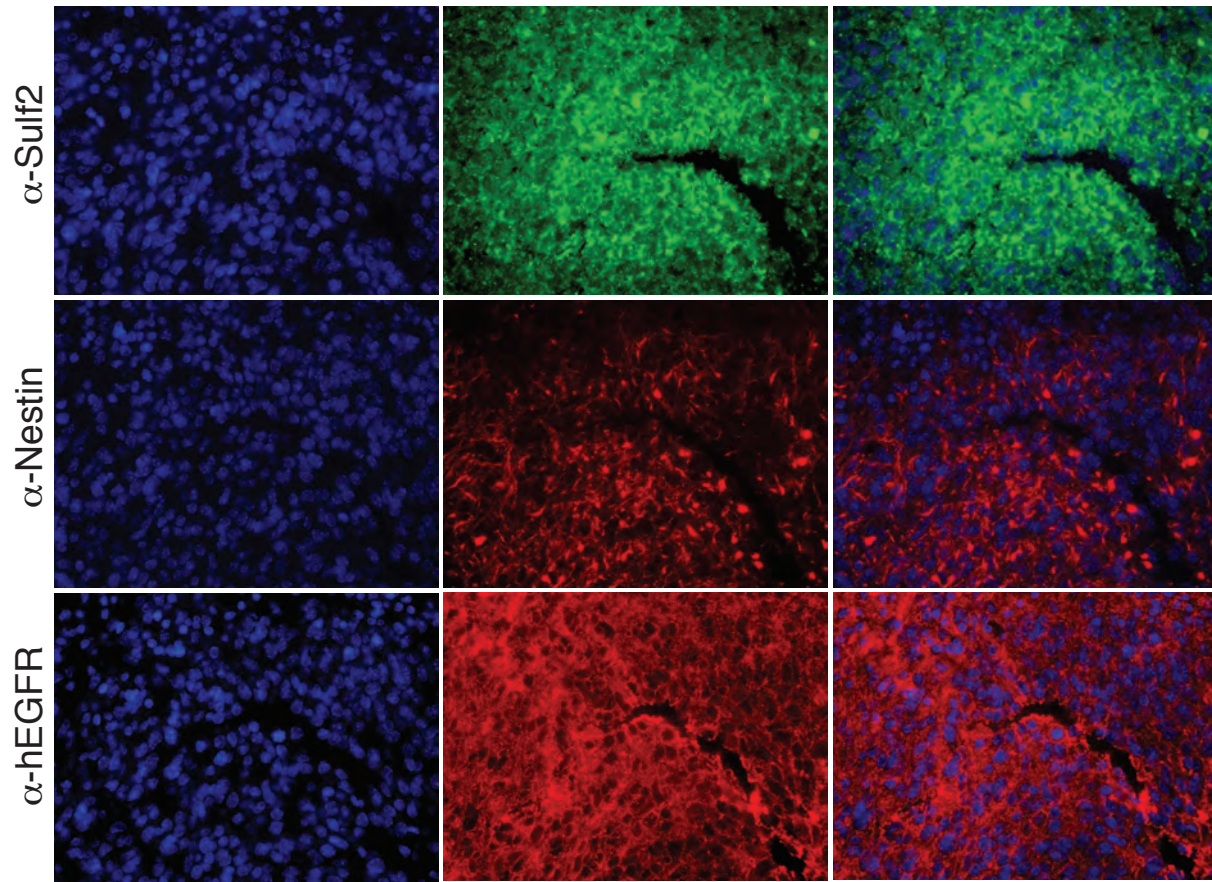
Supplemental Information: This Supplement contains eight Figures and three Tables.



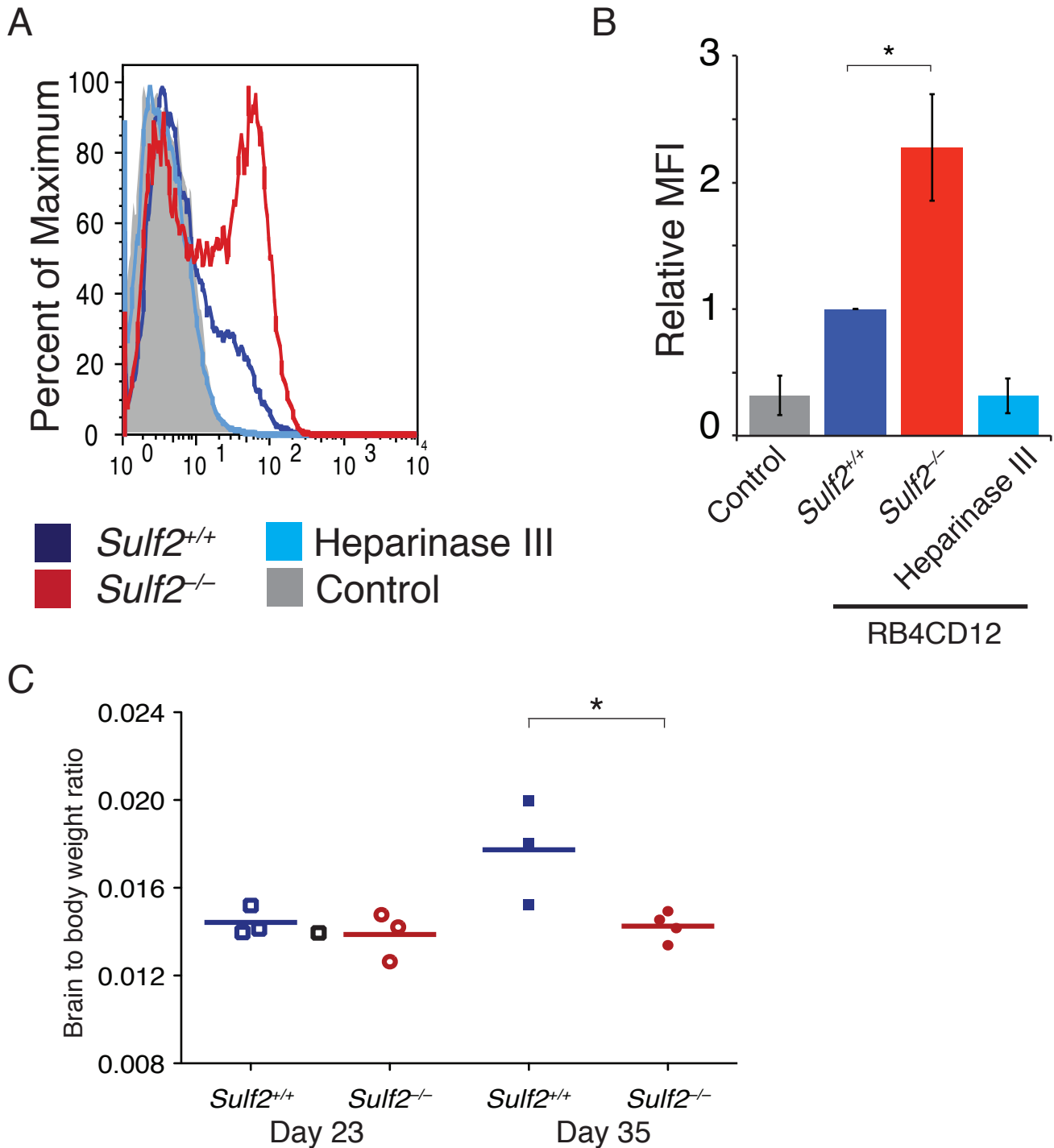
Supplemental Figure 1. Gene amplification of *SULF2* and expression of *WT1* and *TP53* in primary human GBM and human GBM cell lines. (A) Amplification (red) of 20q13.12-q13.13 including the *SULF2* gene in 18 of 372 primary human GBM tumors plotted from low to high expression levels of *SULF2* (x-axis). *SULF2* expression was increased in 11 of these 18 tumors (62%), see Table S1. One of 372 tumors showed deletion (blue) of this region. (B) Relative *WT1* expression in four human glioma cells lines with different expression levels of *SULF2* (Figures 1D) as determined by qRT-PCR. Results are means \pm SEM ($n=3$), $*p<0.005$. (C) Relative expression of *TP53* expression in four human glioma cells lines as determined by qRT-PCR. Results are means \pm SEM ($n=3$), $*p<0.005$. (D) No significant association between expression of *SULF2* and expression of *WT1* in primary human GBM (Pearson correlation coefficient, $r= -0.202$). (E) No significant association between expression of *SULF2* and expression of *TP53* in primary human GBM (Pearson correlation coefficient, $r=0.20$). In silico analysis was performed on expression data from the TCGA Data Portal (2011) for panels (A), (D), and (E). See also Supplemental Table 1 and 2.



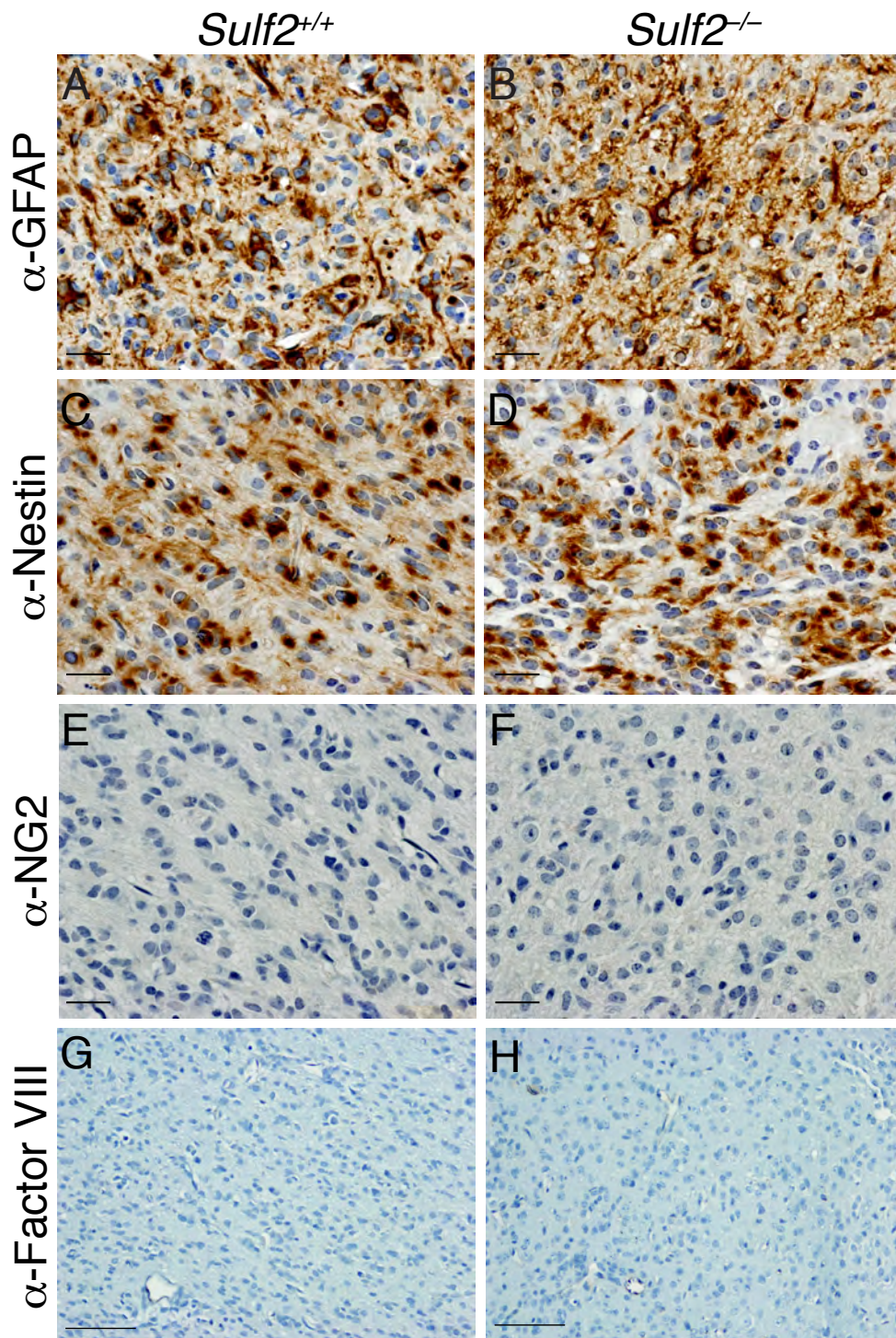
Supplemental Figure 2. SULF2 expression in murine and human tumor cells. (A,C,D) Representative images of murine tumors immunostained for EGFR (A), Olig2 (A, C), Sulf2 (C,D), and GFAP (D). (A) Expression of Olig2 in human EGFR-positive murine tumors. (B) Fraction of OLIG2(+) tumor cells that are also SULF2(+) in murine tumors and in primary human GBM. Mean \pm SEM, n=4 and n=5, respectively. Three to five random fields (400x magnification) were quantified per tumor. (C,D) Dual immunofluorescence in murine tumors demonstrates Sulf2 protein (C and D, green) expression in both Olig2-(C, red) and GFAP-(D, red) positive cells. Scale bar represents 20 μ m (A); original magnification x400 (C) and x630 with oil (D).



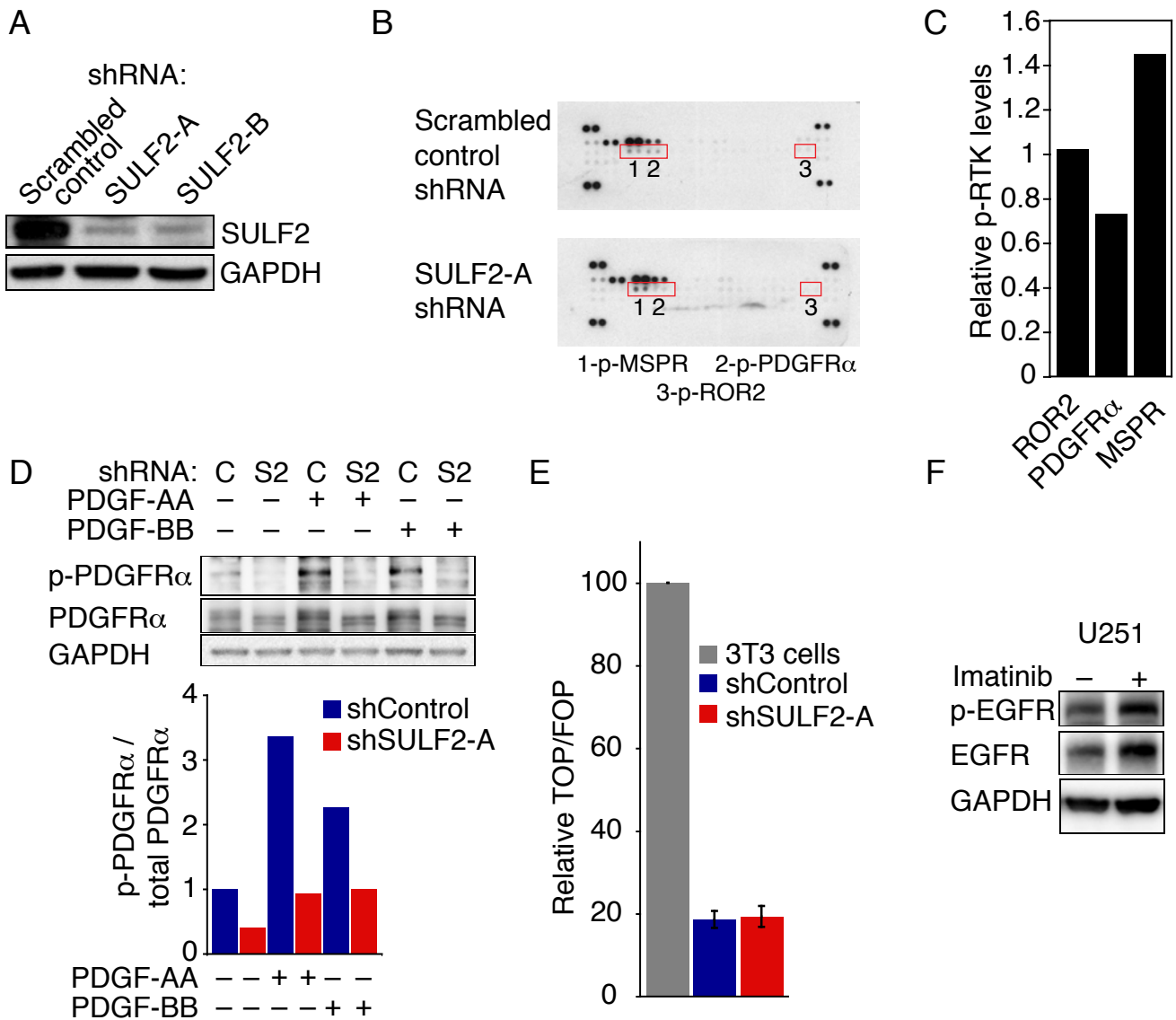
Supplemental Figure 3. Sulf2 expression in murine tumors. Representative serial sections of murine tumors immunostained to highlight hEGFR-positive tumor cells (red, bottom), Sulf2-positive cells (green, top), and Nestin-positive cells (red, middle). In areas with dense tumor and dense Sulf2-positivity a subpopulation of tumors cells appear to also be Nestin-positive. Original magnification x630 with oil. Nuclei are stained with DAPI (blue, left and in merged image on the right).



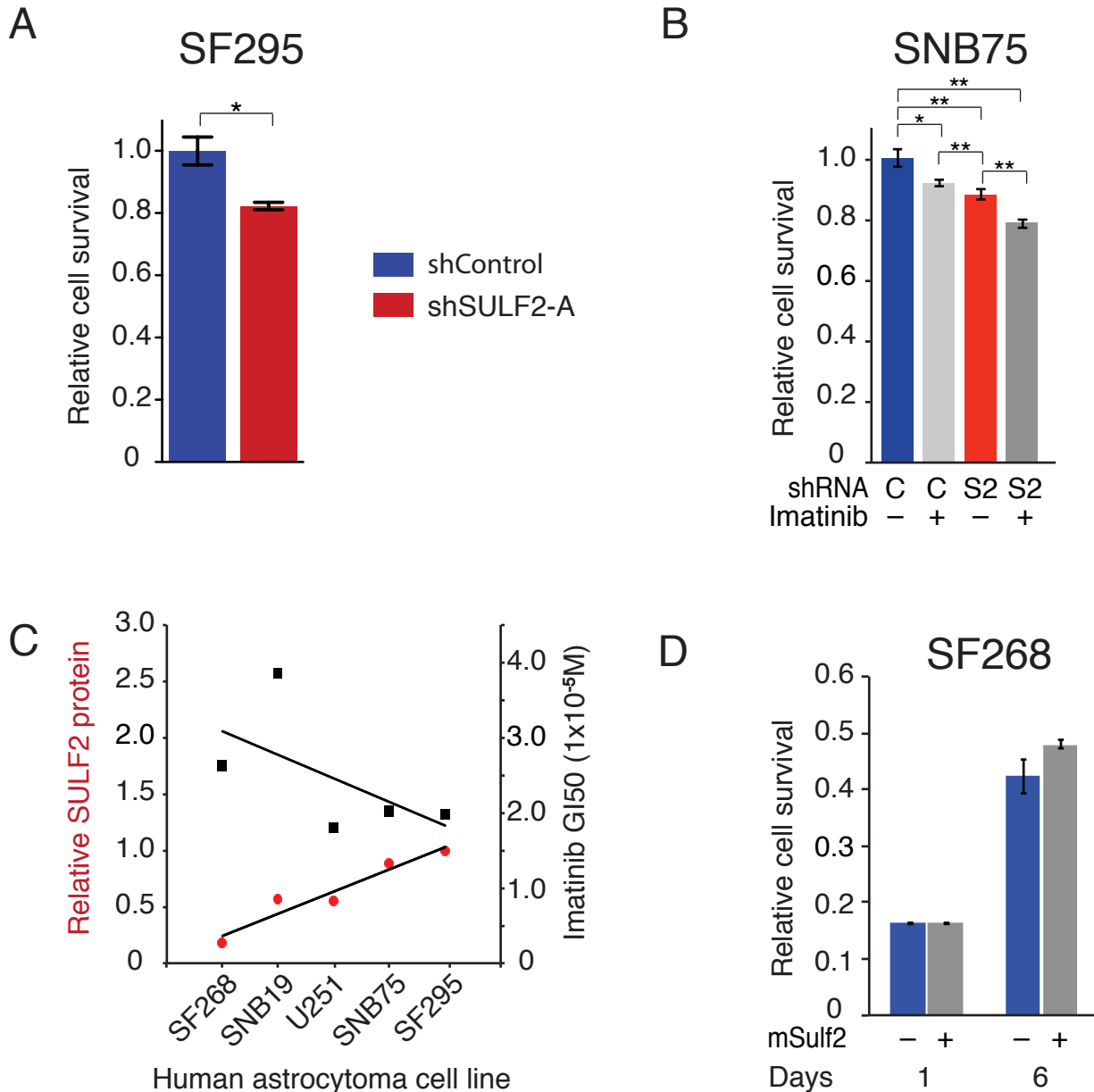
Supplemental Figure 4. *Sulf2*^{-/-} neurospheres have increased levels of cell surface sulfated heparan sulfate proteoglycans and *Sulf2*^{-/-} tumor neurospheres have decreased tumor growth in vivo. (A) Murine *Sulf2*^{+/+} (blue) and *Sulf2*^{-/-} (red) neurospheres were analyzed for staining with RB4CD12, specific to highly sulfated HSPGs. Heparinase III pretreatment destroyed the RB4CD12 epitope (light blue). MPB49, a non-HSPG binding scFv antibody, was used as a negative control (grey shading). Data are representative of two independent determinations. (B) Mean fluorescence intensity (MFI) normalized to RB4CD12 levels on *Sulf2*^{+/+} neurospheres. (**p*<0.05, *n*=2, mean ± SD) Data are derived from two independent determinations. (C) Brain to body weight ratio of mice with *Sulf2*^{+/+} (blue) and *Sulf2*^{-/-} (red) tumors at Day 23 and Day 35. **p*<0.05 (one-way ANOVA, Tukey post hoc test), *n*=3-4 mice per group. Bar denotes mean and black box denotes ratio in normal FVB mice without tumor.



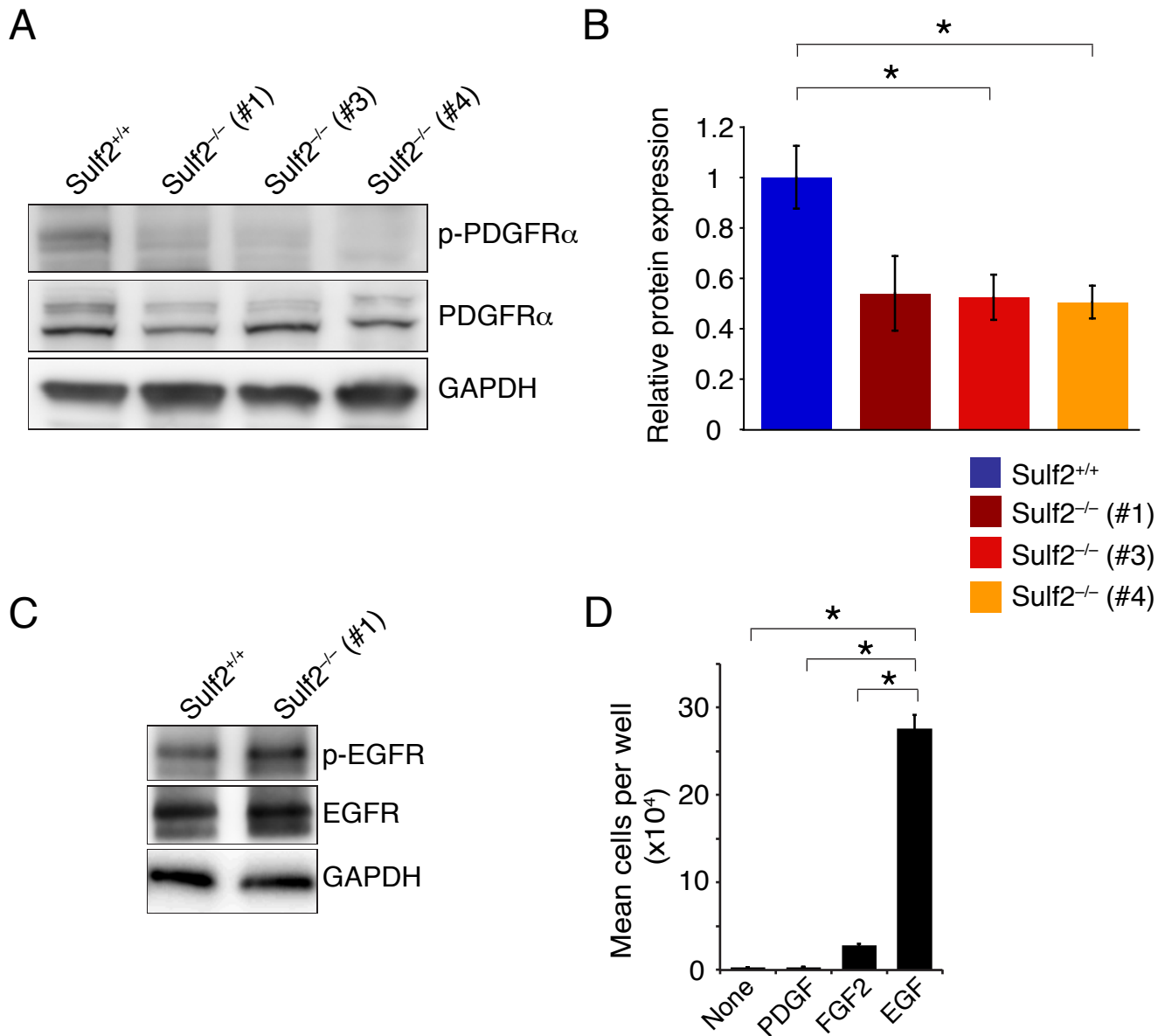
Supplemental Figure 5. *Sulf2*^{+/+} and *Sulf2*^{-/-} tumor progenitors express similar markers of differentiation and similar blood vessel morphology. (A-D) Representative images of GFAP (A, B), Nestin (C, D), NG2 (E, F), and Factor VIII (G-H) immunostaining demonstrating a similar pattern and extent of expression in *Sulf2*^{-/-} and *Sulf2*^{+/+} tumors. Scale bar represents 60 μ m.



Supplemental Figure 6. SULF2 alters the activity of several RTKs in SNB75 cells and alters the responsiveness of U251 cells to PDGF ligands. (A) Efficient knockdown of SULF2 in SNB-75, a human high-grade astrocytoma cell line, by two different shRNA constructs (SULF2-A and SULF2-B) as compared to a scrambled shRNA control (Control). (B) RTK antibody arrays were used to compare RTK activity in protein lysates from SNB75 cells expressing scrambled Control or SULF2-A shRNA. The identity of select RTKs including PDGFR α is indicated. The dark streak at the bottom of the SULF2-A array is an artifact. (C) Relative levels of phosphorylated RTKs in cells with knockdown of SULF2 normalized to the levels in scrambled shRNA Control cells. Duplicate spots were averaged. Cells with knockdown of SULF2 had a 37% decrease in phosphorylated PDGFR α . (D) In U251 cells, knockdown of SULF2 decreases PDGFR α activation in response to PDGF-AA (100 ng/mL) and PDGF-BB (200 ng/mL) stimulation. C=scrambled shRNA control and S2=SULF2-A shRNA. Relative levels of phosphorylated to total PDGFR α are normalized to levels in unstimulated scrambled shRNA control cells. Data is representative of two experiments. (E) SULF2 knockdown has no effect on autocrine Wnt signaling in U251 cells. Mean \pm SEM for three determinations of TOP/FOP activity relative to positive control are shown (%). 3T3 cells expressing Wnt3a were used as a positive control. (F) There was no decrease in levels of phosphorylated EGFR in Imatinib mesylate-treated versus saline treated U251 cells.



Supplemental Figure 7. Tumor cell viability in multiple human astrocytoma cell lines with SULF2 knockdown and overexpression and imatinib-sensitivity and SULF2 protein expression in a subset of NCI-60 cell lines. (A) Knockdown of SULF2 in SF295 cells results in decreased cell viability. * $p < 0.001$, $n = 4$, mean \pm SEM. (B) Knockdown of SULF2 in SNB75 cells in combination with inhibition of PDGFR α by imatinib mesylate (8 μ M) results in decreased cell viability. * $p < 0.001$ and ** $p < 0.0001$, $n = 5$, mean \pm SD. (C) Relative SULF2 protein levels as determined by Western blot (red) and the imatinib growth inhibitory 50 (GI50) dose of imatinib obtained from the NCI-60 Cancer Cell Line Screen (<http://dtp.nci.nih.gov/index.html>). There was a trend between high SULF2 protein levels and increased sensitivity to the PDGFR α inhibitor imatinib ($p < 0.088$, based on linear regression). (D) Overexpression of murine Sulf2 (mSulf2) in SF268 cells trended with increased cell viability. $p = 0.083$, $n = 4$, mean \pm SEM. (A, B, and D) are representative of 2 independent experiments done in quadruplicate. C=scrambled shRNA control and S2=SULF2-A shRNA.



Supplemental Figure 8. Decreased activation of PDGFR α following stimulation with PDGF-BB in *Sulf2*^{-/-} tumor-NS relative to *Sulf2*^{+/+} tumor-NS. (A) Phosphorylated and total PDGFR α levels in *Sulf2*^{+/+} tumor-NS and three independent *Sulf2*^{-/-} tumor-NS lines following stimulation with PDGF-BB (100 ng/mL). Western blots were probed for GAPDH as a loading control. (B) Normalized mean ratio of p-PDGFR α to total PDGFR α levels in tumor-NS from *Sulf2*^{+/+} cells and *Sulf2*^{-/-} cells \pm SEM ($n=3$ independent experiments), $*p<0.05$. (C) Phosphorylated and total EGFR levels in *Sulf2*^{+/+} tumor-NS and *Sulf2*^{-/-} tumor-NS line following stimulation with EGF (20 ng/mL). Western blots were probed for GAPDH as a loading control. (D) Tumor-prone neurospheres, expressing EGFRvIII, are responsive to exogenous growth factor and exhibit increased proliferation in response to EGF. $*p<0.05$, $n=3$ (one-way ANOVA, Tukey post hoc test). Data is representative of two independent experiments.

Supplemental Table 1. GBM with chromosomal alterations encompassing *SULF2* and *SULF2* expression.

Sample ID	Copy number (log₂ ratio)^A	SULF2 gene status^B	<i>SULF2</i> expression (log₂ ratio)^C	<i>SULF2</i> expression relative to normal^D
TCGA-16-0850	-0.86	Deleted	0.415	N
TCGA-26-1799	0.504	Amplified	1.024	Increased
TCGA-02-0083	0.508	Amplified	0.58	N
TCGA-41-2571	0.510	Amplified	2.526	Increased
TCGA-16-1060	0.514	Amplified	1.651	Increased
TCGA-02-0333	0.533	Amplified	0.695	N
TCGA-06-0158	0.554	Amplified	1.356	Increased
TCGA-14-0871	0.555	Amplified	1.18	Increased
TCGA-06-0185	0.556	Amplified	-0.06	N
TCGA-12-3649	0.558	Amplified	1.145	Increased
TCGA-12-3648	0.572	Amplified	1.03	Increased
TCGA-32-2638	0.580	Amplified	1.303	Increased
TCGA-02-2466	0.584	Amplified	0.82	N
TCGA-06-0171	0.664	Amplified	1.145	Increased
TCGA-26-1440	0.664	Amplified	1.735	Increased
TCGA-12-3652	0.671	Amplified	0.241	N
TCGA-32-2634	0.689	Amplified	1.898	Increased
TCGA-14-2555	0.712	Amplified	-0.729	N
TCGA-02-0266	2.629	Amplified	2.503	Increased

^A Copy number data, log₂[Tumor/ Normal], were obtained from TCGA Data Portal, Genome-wide SNP_6.

^B Expression data, log₂[Tumor/ Normal], were obtained from TCGA Data Portal, AgilentG4502A_07.

^C Gene amplification detected in 18 of 372 tumors [log₂(Tumor/Normal) greater than 0.5 (fold-change of copy number in tumor vs. normal greater than or equal to 1.41)].

^D Increased *SULF2* expression detected in 12 of the 18 amplified tumors [log₂(Tumor/Normal) greater than 1.0 (fold-change of expression in tumor vs. normal greater than or equal to 2.0)]. N = not changed.

Supplemental Table 2. SULF2 protein and chromosomal amplification of the SULF2 region in human glioma cell lines.

Cell line	SULF2 amplified^A	Protein by Western blot^B
U87	No	0
U251	No	+
SF295	4 copies	+++
SNB75	No	++

^AThe data were obtained from the Wellcome Trust Sanger Institute Cancer Genome Project web site, <http://www.sanger.ac.uk/genetics/CGP>.

^BRefer to Figure 1D.

Supplemental Table 3. Association of *SULF2* expression with top 50 signature genes per subtype.

Subtype ^A	Signature gene	Pearson Correlation (<i>r</i>) with <i>SULF2</i> expression	Centroid score ^B
Classical	EGFR	-0.115580562	5.557410306
Classical	MEOX2	-0.18968974	3.014033885
Classical	SOCS2	-0.059460725	2.953222174
Classical	NOS2A	-0.117029845	2.704431794
Classical	ELOVL2	-0.311473134	2.643564304
Classical	CDH4	-0.025898981	2.626412667
Classical	KCNF1	-0.110472497	2.595180754
Classical	ACSBG1	-0.144826772	2.240475404
Classical	PDGFA	-0.050653158	2.232093504
Classical	CENTD3	-0.063495567	2.201838057
Classical	GRIK1	-0.129678678	2.178078649
Classical	KLHL4	-0.045487784	2.174396997
Classical	CAMK2B	-0.251183635	2.160479783
Classical	GAS1	-0.012388101	2.157331506
Classical	RGS6	-0.168037199	2.132652475
Classical	VAV3	-0.134790251	2.119220614
Classical	SLC4A4	-0.12377635	2.049291991
Classical	MEIS1	-0.112686958	2.010976325
Classical	FGFR3	-0.263537208	1.924263994
Classical	MYO5C	-0.075010811	1.898741897
Classical	HS3ST3B1	-0.170504343	1.81820168
Classical	GPR17	0.337833577	1.755839546
Classical	DENND2A	0.042729644	1.752964264
Classical	MAB21L1	0.033143909	1.747856699
Classical	TRIB2	0.194131188	1.721138384
Classical	ZFHX4	0.12335461	1.704410394
Classical	KLHDC8A	-0.168182508	1.690371516
Classical	NES	0.177529573	1.636419217
Classical	EYA2	-0.174520861	1.616748766
Classical	WSCD1	0.127540728	1.594705092
Classical	B3GALT1	-0.029169229	1.587450407
Classical	RASGRP1	-0.13247987	1.549222891
Classical	CREB5	0.072331527	1.530386499
Classical	SHOX2	-0.212246211	1.51335036
Classical	SPRY2	-0.057857305	1.513344234
Classical	CDH6	0.022347111	1.505705987
Classical	IRS2	0.127238187	1.487081107
Classical	SOX9	0.030543779	1.467308605
Classical	FZD3	0.069387325	1.466514547
Classical	ACSL3	-0.043629957	1.443933117
Classical	SEMA6D	-0.012327747	1.437743611

Classical	ITGA7	-0.112996902	1.413810109
Classical	ADAM19	-0.095054307	1.399447467
Classical	SLC6A11	-0.117859557	1.394928863
Classical	LFNG	0.003033656	1.392190926
Classical	CDK6	0.028883554	1.377389935
Classical	LMO2	-0.12114917	1.369711994
Classical	ABCD2	-0.185082293	1.367282901
Classical	MLC1	-0.005815782	1.357427737
Classical	TLE2	0.034240989	1.33963465
Proneural	GPR17	0.337833577	5.468432217
Proneural	TMSL8	0.218062933	3.992476825
Proneural	KLRC3	0.333707754	3.936940273
Proneural	DCX	0.27345802	3.919843024
Proneural	PCDH11Y	0.164324563	3.843694578
Proneural	KLRC4	0.34059644	3.665431855
Proneural	NR0B1	0.239943543	3.348768422
Proneural	HRASLS	0.220178912	3.191888842
Proneural	RAB33A	0.185987563	3.117328296
Proneural	ERBB3	0.272117809	3.025219038
Proneural	RP11-35N6.1	0.323955889	2.956078893
Proneural	C20orf42	0.391410317	2.827534384
Proneural	UGT8	0.303314706	2.762886789
Proneural	CA10	0.304483369	2.695186087
Proneural	MYT1	0.383773554	2.586947018
Proneural	SOX10	0.259946971	2.418246562
Proneural	EPHB1	0.34246575	2.294696018
Proneural	GRID2	0.212534666	2.190430493
Proneural	SOX4	0.326747135	2.18410543
Proneural	KLRK1	0.137927876	2.175892231
Proneural	DNM3	0.339316904	2.153731862
Proneural	PAK3	0.108815309	2.134435903
Proneural	CLGN	0.04743658	2.127960561
Proneural	SCN3A	0.329185104	2.074513781
Proneural	SLC1A1	0.292433452	2.07093533
Proneural	CHD7	0.314862649	2.062646657
Proneural	GPR23	0.217000612	2.059646887
Proneural	AMOTL2	0.383961118	2.02534041
Proneural	SATB1	0.265084193	2.011413286
Proneural	PCDH11X	0.106635441	1.996640431
Proneural	CNTN1	0.281942384	1.970974884
Proneural	TMEFF1	0.24358438	1.925661368
Proneural	LRRTM4	0.130090798	1.868378262
Proneural	TOX3	0.238161228	1.861721633
Proneural	NOL4	0.122883595	1.848210821
Proneural	FAM77C	0.255405039	1.84580465
Proneural	WASF1	0.240741833	1.776402216
Proneural	GNG4	0.138203969	1.755488546

Proneural	DGKI	0.226628914	1.74233096
Proneural	NKX2-2	0.341938832	1.727740769
Proneural	C6orf134	0.293701931	1.703958545
Proneural	ZNF804A	0.193486912	1.679547976
Proneural	PDE10A	0.197745443	1.660129159
Proneural	PAK7	0.100741149	1.650662618
Proneural	C1orf106	0.242696835	1.650363925
Proneural	CXXC4	0.239321749	1.64909308
Proneural	CRMP1	0.269479493	1.636938016
Proneural	SOX11	0.162151987	1.635874907
Proneural	IL1RAPL1	0.255292129	1.62095582
Proneural	C1QL1	0.451117724	1.610220205
Neural	AGXT2L1	-0.154322298	4.950872056
Neural	CCK	-0.308846741	4.420416444
Neural	CRYM	-0.21849186	3.530168776
Neural	MYBPC1	-0.2543174	3.419810513
Neural	NTSR2	-0.21421043	3.183636216
Neural	GRM3	-0.110231261	2.735847577
Neural	TMEM144	-0.043114508	2.646316805
Neural	SERPINI1	-0.069491581	2.484323069
Neural	HPCAL4	-0.092219229	2.433494993
Neural	KCNK1	-0.068535967	2.413141749
Neural	GPR22	-0.150291711	2.377145579
Neural	PPP1R1A	-0.059000766	2.374688784
Neural	VSX1	-0.044499747	2.296134779
Neural	HPCA	-0.200663581	2.045566953
Neural	GABRB2	-0.20992257	1.983610681
Neural	FXYD1	-0.239541738	1.932407353
Neural	DHRS9	-0.118513213	1.881227543
Neural	SLCO1A2	-0.040451831	1.848495044
Neural	CPNE6	-0.181551699	1.847891094
Neural	CLCA4	-0.128376956	1.802806021
Neural	ADD3	0.045236404	1.762683649
Neural	GPR17	0.337833577	1.755839546
Neural	FEZF2	-0.180047948	1.74671515
Neural	VIP	-0.302501116	1.693462883
Neural	LOC201229	-0.172957197	1.651231679
Neural	EDG1	-0.110214191	1.588158228
Neural	GRM1	-0.198776306	1.548181069
Neural	CAMK2G	-0.05955756	1.535910757
Neural	NDRG2	-0.105763251	1.535569633
Neural	CA4	-0.233999059	1.53146841
Neural	SNTA1	-0.278179817	1.520110576
Neural	NDP	-0.180389321	1.458907477
Neural	KCNJ3	-0.176486469	1.418070803
Neural	CHN1	-0.197169497	1.407695233
Neural	CRYL1	-0.065669487	1.392508564

Neural	PPP2R5A	-0.015343994	1.303495503
Neural	TSNAX	-0.072581043	1.274972072
Neural	SLC30A10	-0.153321928	1.270285712
Neural	ACYP2	-0.148482602	1.26664105
Neural	ANXA3	-0.171245257	1.23151518
Neural	SEPP1	-0.103398253	1.228340844
Neural	CASQ1	-0.25053016	1.211868428
Neural	FLJ22655	-0.16264993	1.168861631
Neural	IMPA1	-0.029332378	1.163254655
Neural	NSL1	-0.030719377	1.149288597
Neural	ZNF323	-0.155469572	1.118032429
Neural	RBKS	-0.152815882	1.11434835
Neural	YPEL5	-0.059659641	1.111015924
Neural	TTPA	-0.236164581	1.089801257
Neural	SEPW1	-0.125111857	1.089409066
Mesenchymal	LOX	0.138292539	2.914972782
Mesenchymal	FHL2	0.033184578	2.770258389
Mesenchymal	COL1A1	0.155689031	2.63225022
Mesenchymal	COL1A2	0.125393122	2.591322432
Mesenchymal	FCGR2B	0.017669327	2.319804811
Mesenchymal	IGFBP6	-0.052967699	2.31373282
Mesenchymal	AIM1	0.153719687	2.309739855
Mesenchymal	DCBLD2	0.197892058	2.277303553
Mesenchymal	SERPINE1	0.150884473	2.237783994
Mesenchymal	SRPX2	0.099138027	2.188744443
Mesenchymal	LY96	-0.024735736	2.104633625
Mesenchymal	PLAU	0.218392416	2.021120318
Mesenchymal	CLEC2B	0.003640771	2.009015485
Mesenchymal	CSTA	-0.048356069	1.992019483
Mesenchymal	BNC2	0.08522686	1.965290585
Mesenchymal	THBS1	0.193549714	1.951789507
Mesenchymal	RAB27A	0.089739471	1.946635856
Mesenchymal	FPRL2	0.162081323	1.920187975
Mesenchymal	TGFBI	0.193328962	1.905329863
Mesenchymal	COL5A1	0.051150965	1.881686203
Mesenchymal	DSE	0.19815769	1.84810771
Mesenchymal	PLAUR	0.073318973	1.845895497
Mesenchymal	FLJ22662	0.046551246	1.811608378
Mesenchymal	THBD	0.075520512	1.793804547
Mesenchymal	IL1R1	0.154512834	1.759436431
Mesenchymal	GPR17	0.337833577	1.755839546
Mesenchymal	ARPC1B	0.105384681	1.731003747
Mesenchymal	P4HA2	0.095838562	1.701306194
Mesenchymal	LAMB1	0.279607825	1.660408183
Mesenchymal	NCF2	0.069235195	1.65558407
Mesenchymal	TIMP1	-0.003813835	1.616599554
Mesenchymal	MVP	0.188456672	1.609968442

Mesenchymal	IFI30	0.072817462	1.599089189
Mesenchymal	COL8A2	-0.071142475	1.598960055
Mesenchymal	CNN2	0.197359601	1.592983266
Mesenchymal	PSCDBP	0.100033298	1.585668474
Mesenchymal	MAFB	0.174939042	1.529620085
Mesenchymal	SLAMF8	0.022702179	1.528607007
Mesenchymal	FER1L3	0.168843521	1.514002118
Mesenchymal	C5AR1	0.115765433	1.51361621
Mesenchymal	ADAM12	0.136807976	1.512657617
Mesenchymal	S100A11	0.05094748	1.508572836
Mesenchymal	NRP1	0.191873656	1.50556833
Mesenchymal	TNFAIP8	-0.111569624	1.490559773
Mesenchymal	LAIR1	0.085575602	1.483873214
Mesenchymal	CTSC	0.170917228	1.468256675
Mesenchymal	LY75	0.08502604	1.448435602
Mesenchymal	C1orf38	0.135222625	1.447385433
Mesenchymal	SQRDL	0.004945795	1.439821301
Mesenchymal	CTSB	0.203689138	1.428534927

^ATop 50 signature genes were defined based on centroid score (8). Pearson correlation calculated on normalized expression data from TCGA Data Portal (85), Affymetrix Human Exon 1.0 ST microarray platform on 202 human GBM tissue samples.

^BCentroid score from (8).